



저작자표시-비영리-동일조건변경허락 2.0 대한민국

이용자는 아래의 조건을 따르는 경우에 한하여 자유롭게

- 이 저작물을 복제, 배포, 전송, 전시, 공연 및 방송할 수 있습니다.
- 이차적 저작물을 작성할 수 있습니다.

다음과 같은 조건을 따라야 합니다:



저작자표시. 귀하는 원저작자를 표시하여야 합니다.



비영리. 귀하는 이 저작물을 영리 목적으로 이용할 수 없습니다.



동일조건변경허락. 귀하가 이 저작물을 개작, 변형 또는 가공했을 경우에는, 이 저작물과 동일한 이용허락조건하에서만 배포할 수 있습니다.

- 귀하는, 이 저작물의 재이용이나 배포의 경우, 이 저작물에 적용된 이용허락조건을 명확하게 나타내어야 합니다.
- 저작권자로부터 별도의 허가를 받으면 이러한 조건들은 적용되지 않습니다.

저작권법에 따른 이용자의 권리는 위의 내용에 의하여 영향을 받지 않습니다.

이것은 [이용허락규약\(Legal Code\)](#)을 이해하기 쉽게 요약한 것입니다.

[Disclaimer](#)

공학석사학위논문

**Fatigue Assessment of Sign Structures
for Truck-Induced Gusts**

트럭풍 거스트에 대한
표지판 구조의 피로평가

2015년 2월

서울대학교 대학원
건설환경공학부
한 성 욱

**Fatigue Assessment of Sign Structures
for Truck-Induced Gusts**
트럭풍 거스트에 대한
표지판 구조의 피로평가

지도교수 김 호 경




이 논문을 공학석사학위논문으로 제출함

2015 년 2 월

서울대학교 대학원
건설환경공학부
한 성 욱

한성욱의 공학석사 학위논문을 인준함

2015 년 2 월

위 원 장	<u>고 호 경</u>	
부위원장	<u>김 호 경</u>	
위 원	<u>송 준 호</u>	

ABSTRACT

In this thesis, a fatigue assessment was performed for structural support such as highway signs, luminaires, and traffic signals. A particular focus was on truck-induced gusts that occur when trucks pass beneath a structure in order to estimate whether fatigue stress due to truck-induced gusts is larger than the threshold stress or not. Because it is difficult to simulate truck-induced gusts in a wind-tunnel test, this research was carried out through field tests. The target of the field tests was involved the use of a variable message sign (VMS) which is subjected to the biggest fatigue stress according to the AASHTO due to its large projected area in the horizontal plane.

Three types of the sensors were used in the field tests with a focus on the fatigue-critical part which is the lower mast arm. Three and eight strain gauges were installed on the bottom and the front of the mast arm, respectively, in order to estimate the range of the fatigue stress. Three pressure sensors were installed on the bottom and the front of the VMS, respectively, to understand the characteristics of truck-induced gusts and an anemometer was installed at the same height of the VMS for use in distinguishing the effects between truck-induced gusts and natural wind gusts.

Measured nominal stress was calculated in order to obtain the fatigue stress range by the rainflow counting algorithm and compared with the threshold stress suggested by details of the fatigue-critical part according to the AASHTO. In

addition, the characteristics of truck-induced gusts, as analyzed from measured wind pressure data, were verified through data from both wind pressure gauges and strain gauges.

The measured fatigue stress range was compared with an equivalent static gust pressure. In other words, the equivalent static gust pressure which accounts for the measured fatigue stress range was inversely calculated and compared with the design value for fatigue wind loads suggested the AASHTO.

During the field tests, truck-induced gusts were only estimated because the high wind velocity was not measured. However, if the a larger fatigue stress range had occurred when effect of natural wind gusts was added to truck-induced gusts, it became necessary to analyze the effect of natural wind gusts in a subsequent research.

Keywords: Fatigue assessment, Truck-induced gust, Field test, Structural support, Rainflow counting algorithm

Student Number: 2013-20948

TABLE OF CONTENTS

ABSTRACT	I
TABLE OF CONTENTS	III
LIST OF FIGURES	VI
LIST OF TABLES	VIII
CHAPTER 1	1
INTRODUCTION	1
CHAPTER 2	4
DESIGN SPECIFICATIONS FOR TRUCK-INDUCED GUSTS	4
2.1 AASHTO	4
2.2 DMRB	6
CHAPTER 3	8
PREPARATION OF THE FIELD TEST	8
3.1 SITE OF THE FIELD TEST	8
3.2 TARGET OF THE FIELD TEST	9
3.3 FATIGUE ANALYSIS FOR THE FATIGUE-CRITICAL PARTS	12
3.4 MEASUREMENT SENSORS	16

3.4.1 Wind pressure	17
3.4.2 Strain	19
3.4.3 Wind velocity	22
CHAPTER 4	24
CHARACTERISTICS OF TRUCK-INDUCED GUSTS	24
4.1 WIND PRESSURE OF TRUCK-INDUCED GUSTS	24
4.2 DISTRIBUTION OF TRUCK-INDUCED GUSTS	26
CHAPTER 5	30
FATIGUE ASSESSMENT	30
5.1 RAINFLOW COUNTING ALGORITHM.....	30
5.2 NOMINAL STRESS POINT	31
5.3 MEASUREMENT RESULT.....	33
5.4 VERIFICATION OF THE DISTRIBUTION OF TRUCK-INDUCED GUSTS	37
CHAPTER 6	40
COMPARISON BETWEEN AASHTO AND MEASUREMENT RESULTS.....	40
6.1 EQUIVALENT STATIC GUST PRESSURE OF BOTH THE FRONT AND BOTTOM SURFACE.....	40
CHAPTER 7	42

FURTHER STUDIES	42
7.1 WIND PRESSURE OF THE VMS REAR SURFACE.....	42
7.2 FATIGUE ASSESSMENT ABOUT NATURAL WIND GUSTS.....	42
CHAPTER 8	44
CONCLUSIONS.....	44
REFERENCES	46
국 문 초 록.....	48

LIST OF FIGURES

FIG. 3.1 A SKY VIEW OF THE SITE	9
FIG. 3.2 THE TARGET OF THE FIELD TEST	10
FIG. 3.3 REAR AND SIDE VIEWS OF THE VMS STRUCTURE	11
FIG. 3.4 TOP VIEW OF THE VMS STRUCTURE	11
FIG. 3.5 FATIGUE-CRITICAL PARTS OF THE FIELD TEST TARGET	13
FIG. 3.6 EXAMPLE FOR THE DETAIL OF FATIGUE-CRITICAL PART	15
FIG. 3.7 SENSORS USED FOR THE FIELD TESTS	17
FIG. 3.8 WIND PRESSURE SENSORS USED FOR THE FIELD TESTS	18
FIG. 3.9 STRAIN GAUGES USED FOR THE FIELD TESTS	20
FIG. 3.10 STRESS DISTRIBUTION RESULT FROM THE NCHRP PROJECT 10-70	21
FIG. 3.11 STRESS DISTRIBUTION RESULT FROM THE ABAQUS ANALYSIS	22
FIG. 3.12 PICTURES OF THE INSTALLED ANEMOMETER	23
FIG. 4.1 TIME HISTORY OF WIND PRESSURES INSTALLED ON THE FRONT OF THE VMS	25
FIG. 4.2 TIME HISTORY OF WIND PRESSURES INSTALLED AT THE BOTTOM OF THE VMS AND ON THE FRONT OF THE VMS	25
FIG. 4.3 WIND PRESSURE SENSOR 1, 2 AND 3	26
FIG. 4.4 DESCRIPTION OF THE TWO CASE FOR ANALYZING DISTRIBUTION OF TRUCK-INDUCED GUSTS	27
FIG. 4.5 REDUCTION RATIO OF WIND PRESSURE WHEN A TRUCK PASSES BENEATH THE VMS STRUCTURE	28
FIG. 4.6 EXAMPLE FOR DISTRIBUTION OF WIND PRESSURE OCCURRED BY TRUCK-INDUCED GUSTS	29

FIG. 5.1 STRESS RATIO ACCORDING TO THE DISTANCE FROM THE STIFFENERS	32
FIG. 5.2 DESCRIPTION ABOUT THE DISTANCE FROM THE STIFFENERS	32
FIG. 5.3 CYCLES OF FATIGUE STRESS RANGES MEASURED ON THE FRONT OF THE MAST ARM...	34
FIG. 5.4 CYCLES OF FATIGUE STRESS RANGES MEASURED AT THE BOTTOM OF THE MAST ARM.	35
FIG. 5.5 TIME HISTORY GRAPH OF SENSORS WHEN THE MAXIMUM STRESS RANGE WAS OCCURRED	36
FIG. 5.6 TIME HISTORY DATA USED FOR VERIFICATION OF DISTRIBUTION OF TRUCK-INDUCED GUSTS	37

LIST OF TABLES

TABLE 2.1 FATIGUE IMPORTANCE FACTORS, I_F	5
TABLE 3.1 PROPERTIES OF THE SITE.....	9
TABLE 3.2 RESULTS OF FATIGUE ANALYSIS	15
TABLE 5.1 RESULT OF FATIGUE STRESS RANGE CALCULATED FROM TWO SENSORS	38
TABLE 6.1 COMPARISON BETWEEN MEASURED RESULTS AND THE AASHTO DESIGN VALUE...	40

CHAPTER 1

INTRODUCTION

Structural supports such as highway signs, luminaires, and traffic signals are simple structures that are commonly seen. Although these are not complex structures such as long span bridges, they are vulnerable to fatigue failure. Up to now, examples of fatigue failure have been reported and this phenomena is frequently seen during periods of strong winds.

To design the structural supports for these structures, fatigue design as well as structural design should be considered. Design criteria such as AASHTO, DMRB, Eurocode recommend equivalent static fatigue loads for various situations, while domestic design criteria do not consider fatigue failure. This design criteria suggests that galloping, vortex-induced vibration, truck-induced gust, natural wind gust are the main causes of fatigue failure. Although both galloping and vortex-induced vibrations during the four reasons generate a larger stress than truck-induced gusts and natural wind gusts, the repetition rate of galloping and vortex-induced vibrations is relatively lower than the other two phenomena.

Preliminary studies (Albert et al. 2007) have shown that truck-induced gusts generally generate the lowest stress among the four primary reasons and structural supports which satisfy the fatigue designs for natural wind gusts are automatically included in the fatigue design criteria for truck-induced gusts. Truck-induced gusts

are generated when a truck passes beneath a structural support and gust loads induced due to the passage of trucks by attachments mounted to the horizontal support of the structure (AASHTO 2013). The AASHTO especially mentions that the critical direction for applying gust loads is the exposed horizontal surface of the attachment and the horizontal support. In particular, variable message sign (VMS) structures which have large projected areas in the horizontal plane are reported to be particularly sensitive to truck-induced gusts.

Unlike the AASHTO or other design specifications, there are no design specifications for the fatigue design of structural supports in this country. It is necessary to check how structural supports in the country are stable against fatigue failure. Moreover, the design standards for structural supports varies from country to country. However, preliminary studies point to improvements that could be applied to structural supports in this country. First point is that most preliminary studies (Johns, Dexter 1998) were carried out using a small number of samples. Considering the characteristics of our country, the rate of heavy vehicle transport is high compared to other countries. The second reason is that types of structural supports are different from one country to another and this is reflected in their one design specifications. So it is necessary to understand the characteristics of structural supports in a country in order to apply alternate design specifications.

Field tests should be carried out to verify the effect of truck-induced gusts due to difficulty of simulating truck-induced gusts in wind-tunnel tests. The site used in the field tests was selected considering vehicle speed, traffic volume and the

characteristics of the structural support. The focus of this thesis was on truck-induced gusts and effect of the truck-induced gusts on the stability of VMS structured was estimated.

CHAPTER 2

DESIGN SPECIFICATIONS FOR TRUCK- INDUCED GUSTS

2.1 AASHTO

The AASHTO, which is standard specifications for structural supports for highway signs, luminaries, and traffic signals has published recommended criteria for fatigue design and states that galloping, vortex-induced vibrations, natural wind gusts and truck-induced gusts are the four main reasons for causing fatigue failure. In particular, the AASHTO suggests an equivalent static truck gust pressure range like below Eq. 2.1.

$$P_{TG} = 900C_d \left(\frac{V_T}{30 \text{ m/s}} \right)^2 \times I_F \quad (\text{Pa}) \quad (2.1 \text{ a})$$

$$P_{TG} = 18.8C_d \left(\frac{V_T}{65 \text{ mph}} \right)^2 \times I_F \quad (\text{psf}) \quad (2.1 \text{ b})$$

V_T is truck speed and C_d and I_F are drag coefficient and fatigue importance factor, respectively. The drag coefficient for VMS is 1.7 suggested by the

AASHTO. Recommended fatigue importance factors are 0.3 – 1.0, depending on both types of structures and the location where the structures are installed. Fatigue importance factors are shown below in Table. 2.1 (AASHTO 2013) and structures classified as category I mean a high hazard in the event of failure when the truck speed exceeds 60 km/h and the average daily traffic (ADT) exceeds 10,000 or the average daily truck traffic (ADTT) exceeds 1,000. Because the target for field tests is classified as category I, 1.0 was used for field tests.

Table 2.1 Fatigue importance factors, I_F

Fatigue importance category			Galloping	Natural wind gusts	Truck-induced gusts
Cantilevered	I	Sign	1.0	1.0	1.0
		Traffic signal	1.0	1.0	1.0
	II	Sign	0.70	0.85	0.90
		Traffic signal	0.65	0.80	0.85
	III	Sign	0.40	0.70	0.80
		Traffic signal	0.43	0.55	0.70
Noncantilevered	I	Sign	-	1.0	1.0
		Traffic signal	-	1.0	1.0
	II	Sign	-	0.85	0.90
		Traffic signal	-	0.80	0.85
	III	Sign	-	0.70	0.80
		Traffic signal	-	0.55	0.70

The AASHTO suggests this equation based on 108 km/h, which is a function of truck speed. Equivalent static truck gust pressure is proportional to the square of

the ratio between the truck speed and 108 km/h. Therefore, if a truck speed is less than 108 km/h, the equivalent static truck gust pressure can be reduced.

The direction of the equivalent static truck gust pressure range is vertical to the horizontal support like mast arms as well as the area of all signs, attachments, walkways and/or lighting fixtures projected on a horizontal plane. The part of the structures not located directly above a traffic lane is also excluded as a target of truck-induced gusts. Truck-induced gusts are restricted to apply only to a structure where the height of the structure is more than 3 m and less than 7 m. This height range can create the maximum fatigue stress range and truck-induced gusts are fully applied for heights up to and including 6 m. This wind pressure is linearly reduced for heights above 6 m to a value of zero at a height of 10 m.

Because truck-induced gusts are estimated to be the most insignificant fatigue design load among the four fatigue design loads, the AASHTO suggests that truck-induced gust loading can be excluded unless required by the designer. However the AASHTO emphasizes that recent vibration problems due to truck-induced gusts on sign structures with large projected areas in the horizontal plane, such as variable message sign (VMS) enclosures have caused attention to be focused on vertical gust pressures.

2.2 DMRB

Unlike the AAHSTO, the Design Manual for Road and Bridge (DMRB)

suggests truck-induced gusts in both vertical and horizontal directions. Truck-induced gusts are referred to as high vehicle buffeting in the DMRB and the pressure P_d due to high vehicle buffeting is using Eq. 2.2, below.

$$P_d = 600h^{-0.25} - 400 \quad (\text{MPa}) \quad (2.2)$$

The 'h' denotes either the distance from the top of the high sided vehicle to the underside of any horizontal surface or the distance from the top of a high sided vehicle to the center of pressure of any vertical surface. This Equation is applied for values of up to 5 m and applied loads can be calculated as the product of the appropriate pressure and projected area.

CHAPTER 3

PREPARATION OF THE FIELD TEST

3.1 Site of the field test

The site of the field tests was selected considering vehicle speed, the characteristics of VMS structures and the accessibility of VMS structures. Because the static equivalent pressure of truck-induced gusts is a function of vehicle speed according to the AASHTO, the preferred site was a highway. Because VMS structures are also installed at entrances to highways according to need, the section of a highway where VMS structures are installed was investigated. Among the investigated sections of a highway, several sections were sorted by maximum vehicle speed which was surveyed by the Korea Express Corporation. A number of highway lanes was considered so as to prevent the occurrence of traffic jams. Vehicle type was also considered because box-type dump trucks are known to generate the greatest stress (Albert, 2006). Finally, the characteristics of VMS structures were investigated through field investigations to check the size of the mast arm and to determine how many highway lanes affect the mast arm.

The site from the Ansan jct. to the Palgok jct. in The Seohaean expressway was finally selected as the site for the field test. Especially, large-sized buses and box-type dump trucks pass through this section, due to its proximity to the harbor.

Table. 3.1 and Fig. 3.1 show the properties and a view of the site fro above, respectively.

Table 3.1 Properties of the site

No. of lanes (both ways)	Bus (ADTT)	Truck (ADTT)	Mean vehicle speed	Maximum vehicle speed
6	1,750	2,534	92.8 km/h	103.5 km/h



Fig. 3.1 A sky view of the site

3.2 Target of the field test

The target of the field tests was select as VMS structures because it is known as the most vulnerable structure to truck-induced gusts and is shown in Fig. 3.1 as a

red circle. Because there are no standard designs for VMS structures in the country, it was necessary to measure the size of the VMS structures prior to the field tests and the measurements were compared with values from blueprints.

The type of the VMS structure is a cantilevered structure and the mast arms are extended from third lane to second-half lane. The VMS structure is located in a downhill road and below Fig. 000 shows the field test target.



Fig. 3.2 The target of the field test

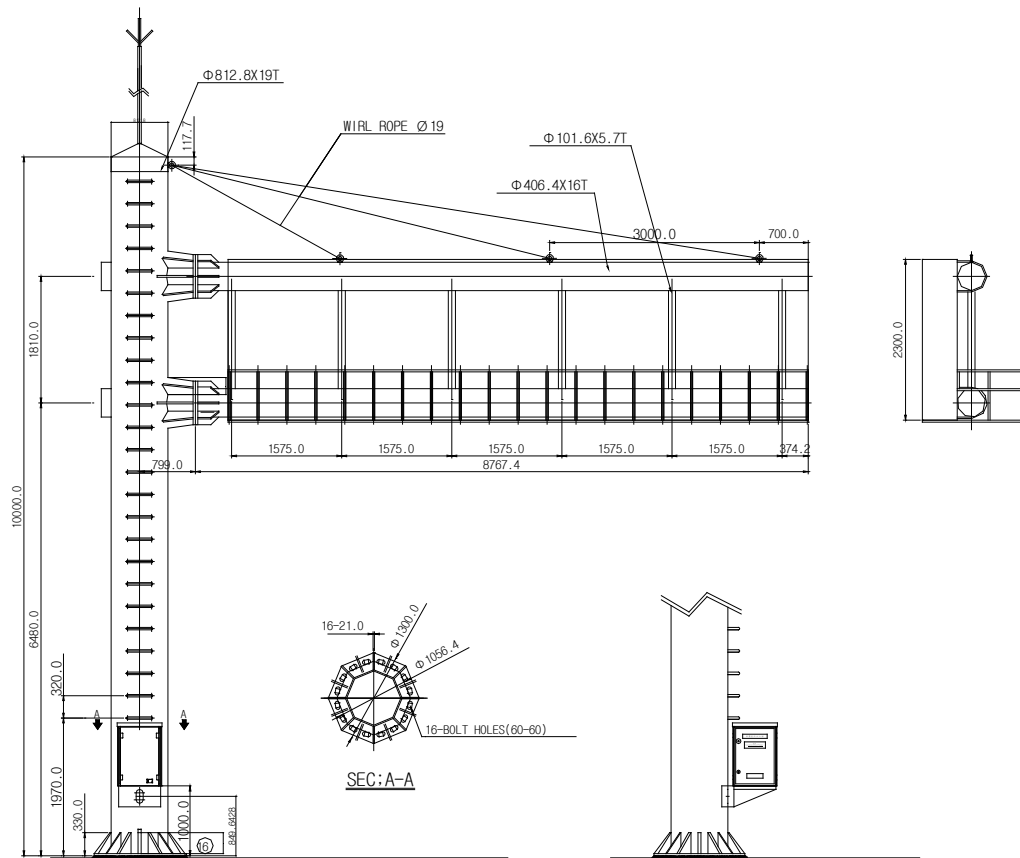


Fig. 3.3 Rear and side views of the VMS structure

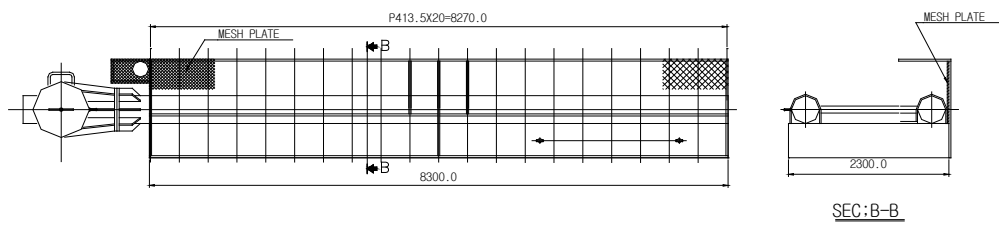


Fig. 3.4 Top view of the VMS structure

The blueprints of the field test target are shown in both Fig. 3.3 and Fig. 3.4. The size of the VMS is 8.3 m × 2.3 m × 0.5 m (width × height × depth) and installation height of the VMS from the ground is about 7.4 m.

3.3 Fatigue analysis for the fatigue-critical parts

A fatigue analysis was carried out regarding the fatigue-critical parts which are the connections between the mast arm and column and between the column and base plate, as shown in Fig. 3.5.

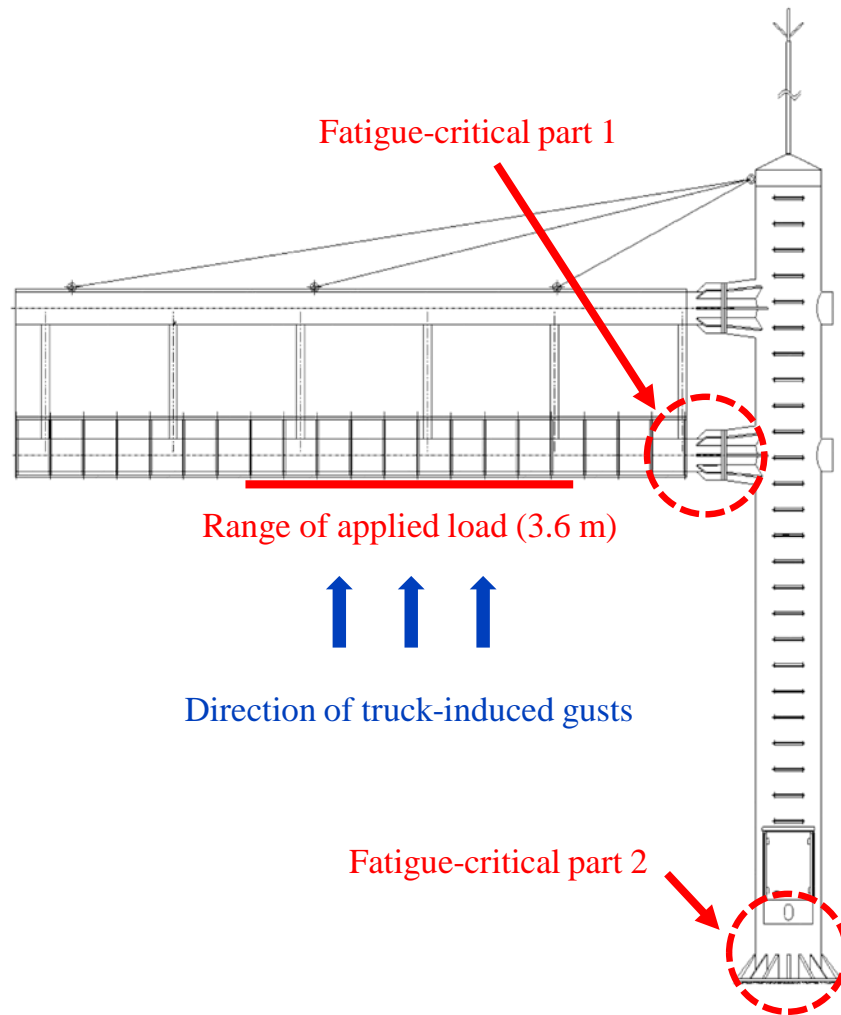


Fig. 3.5 Fatigue-critical parts of the field test target

AASHTO suggests a threshold stress of 48 MPa for fatigue-critical parts that are classified as Category D. The equivalent static wind pressure for natural wind gusts and truck-induced gusts was applied according to the AASHTO. Although the AASHTO suggests the range of the applied load to be 3.7m where truck-induced

gusts are applied, truck-induced gusts were applied to the entire exposed horizontal surface of the attachment and horizontal support. It was therefore assumed that two trucks could pass simultaneously beneath the VMS structures and the maximum fatigue stress range was estimated irrespective of whether it was bigger than the threshold stress or not.

Among the two fatigue-critical parts, the greatest fatigue stress was found to occur in the connection between the mast arm and column. This fatigue-critical part corresponds to section 6 of the fatigue details that the AAHSTO suggests and is defined as a tube-to-transverse-plate connection stiffened by longitudinal attachments with fillet welds in which the tube is subjected to longitudinal loading and the welds are wrapped around the attachment termination. An example for this is shown in Fig. 3.6 and the red lines in Fig. 3.6 indicate the expected fatigue failure line.

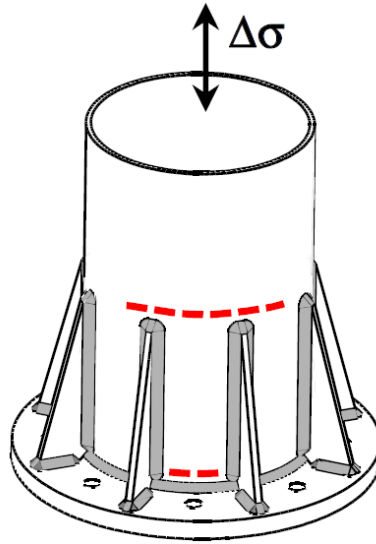


Fig. 3.6 Example for the detail of fatigue-critical part

Table 3.2 Results of fatigue analysis

Fatigue-critical part	Load	Fatigue stress range (MPa)	Threshold stress (MPa)
1	Truck-induced gust	12.9	48.0
2	Truck-induced gust	2.3	48.0
1	Natural wind gust	12.0	48.0

Fatigue analysis results are summarized in Table 3.2. The maximum fatigue stress range that is generated in the connection between the mast arm and column due to truck-induced gusts is 12.9 MPa and is generated in the connection between the column and base plate due to truck-induced gusts is 2.3 MPa. The maximum

fatigue stress range generated in the connection between the mast arm and column due to natural wind gusts is about 12.0 MPa. Therefore, truck-induced gusts generate a maximum fatigue stress range in the VMS structure and the field tests were focused on the connection between the mast arm and column.

3.4 Measurement sensors

The field tests were carried out to evaluate the effects of truck-induced gusts. The fatigue stress range in the connection between the mast arm and column was estimated using strain gauges. The distribution of truck-induced gusts applied to the front and bottom of the VMS were also estimated using pressure sensors. Natural wind gusts as well as truck-induced gusts were also estimated using an anemometer. All of the sensors used are shown in Fig. 3.7.

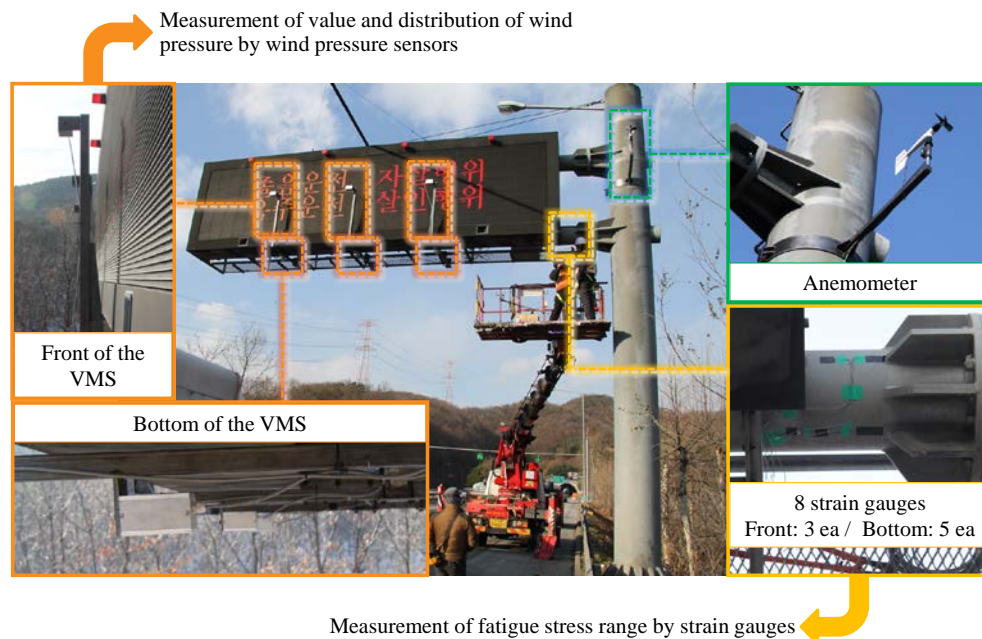


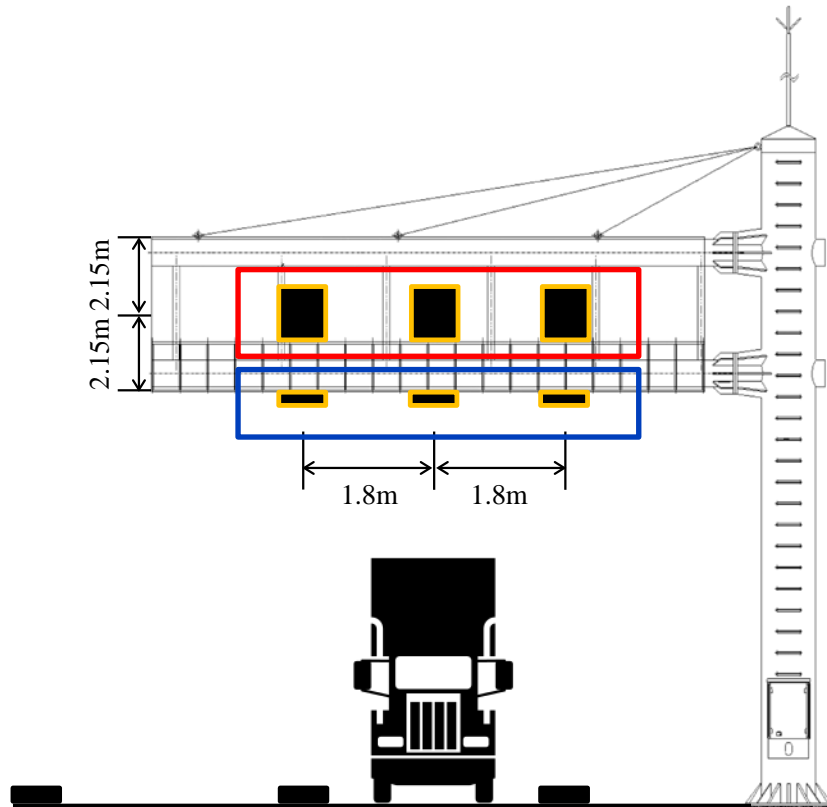
Fig. 3.7 Sensors used for the field tests

All of the sensors were waterproof and functioned 24 hours a day. Data were collected as 100 sampling frequency via a commercial program which is the R-DAS.

3.4.1 Wind pressure

Six wind pressure sensors were used to estimate the distribution of wind pressure due to truck-induced gusts as shown in Fig. 3.8. The AASHTO suggests that truck-induced gusts are only applied to the exposed horizontal surface of an attachment and the horizontal support because the wind pressure of the front surface of the VMS where loads are applied in a horizontal direction is relatively

insignificant compared to natural wind gusts according to the AASHTO.



(a) Sketch of the wind pressure sensors



(b) Pictures of the installed wind pressure sensors

Fig. 3.8 Wind pressure sensors used for the field tests

It is necessary to check how much wind pressure is generated from truck-induced gusts affects to the front surface of the VMS. Three wind pressure sensors were installed in front of the VMS and the other three wind pressure sensors were installed at the bottom of the VMS, as shown in Fig. 3.8.

The three wind pressure sensors were installed at the middle height of the VMS which is 1.15 m from the bottom of the VMS and were used for estimating effects of natural wind gusts and truck-induced gusts to the front of the VMS. The other three wind pressure sensors were installed at the middle bottom of the VMS. The distance between the three sensors was 1.8 m, respectively which is half of one lane width and a sensor in the middle among the three sensors is on the middle of the three-lane.

3.4.2 Strain

A total of eight strain gauges were used to check the fatigue strain range as shown in Fig. 3.9.

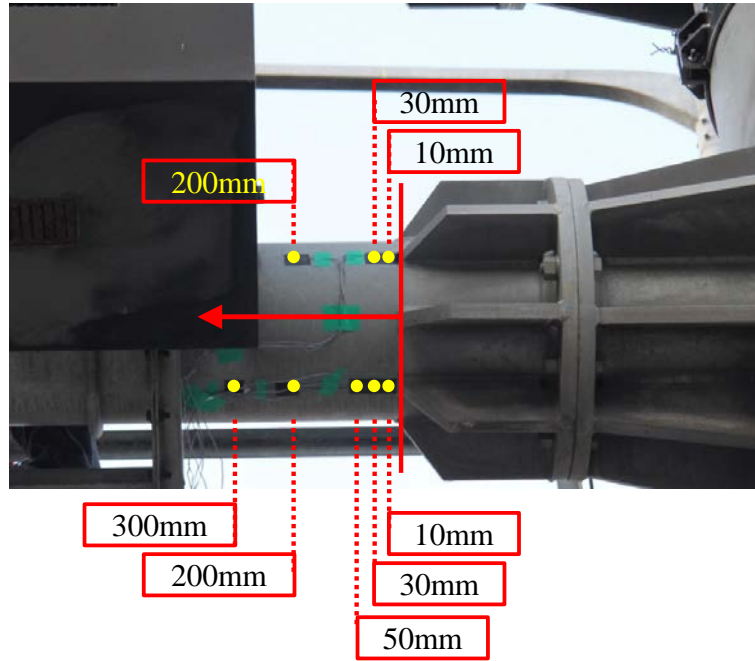


Fig. 3.9 Strain gauges used for the field tests

The main mode directions of the VMS structure are in both the horizontal and vertical directions. Horizontal support vibrations caused by forces due to truck-induced gusts are known as the most critical factor according to the AASHTO. The five strain gauges were installed at the bottom of the under mast arm where the maximum fatigue stress is generated. The other three strain gauges were installed on the front of the mast arm.

The distance between the strain gauges was determined taking stress into consideration. According to the NCHRP Project 10-70, stress can be generated as far away as half of the steel tube outer diameter as shown in Fig. 3.10.

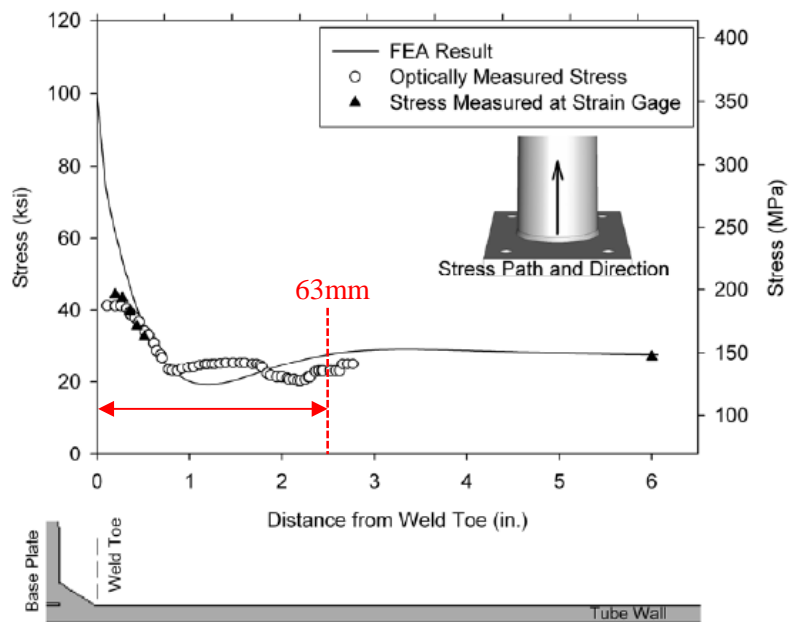


Fig. 3.10 Stress distribution result from the NCHRP Project 10-70

A structural analysis by ABAQUS was also performed for checking the stress that the VMS structure was subjected to, as shown in Fig. 3.11. This result is similar with that of the NCHRP Project 10-70 in which stress can appear as far away as the half of the steel tube outer diameter

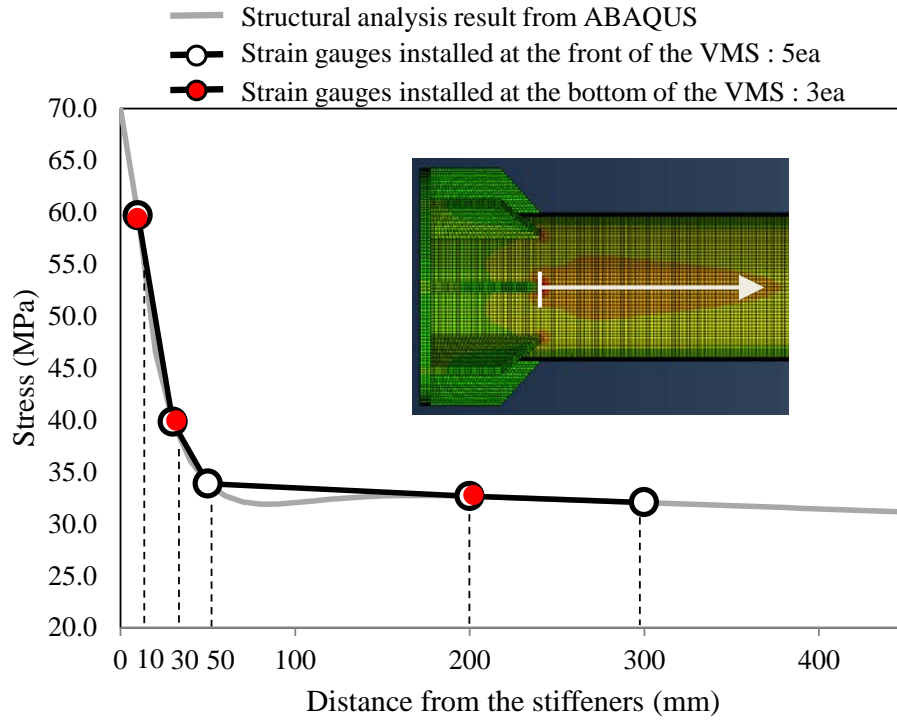


Fig. 3.11 Stress distribution result from the ABAQUS analysis

The five strain gauges shown as white circles in Fig. 3.11 were installed at 10 mm, 30 mm, 50 mm, 200 mm, 300 mm away from the fillet-weld between the mast arm and the stiffener. The other three strain gauges shown as red circles in Fig. 3.11 were installed at 10 mm, 30 mm, 200 mm away from the fillet-weld between the mast arm and the stiffener.

3.4.3 Wind velocity

Wind velocity was measured to estimate the effects of natural wind gusts. It

was utilized to distinguish the effects on the front of the mast arm caused by truck-induced gusts versus that from natural wind gusts. It was also used to check the effect natural wind gusts on the front of the mast arm.

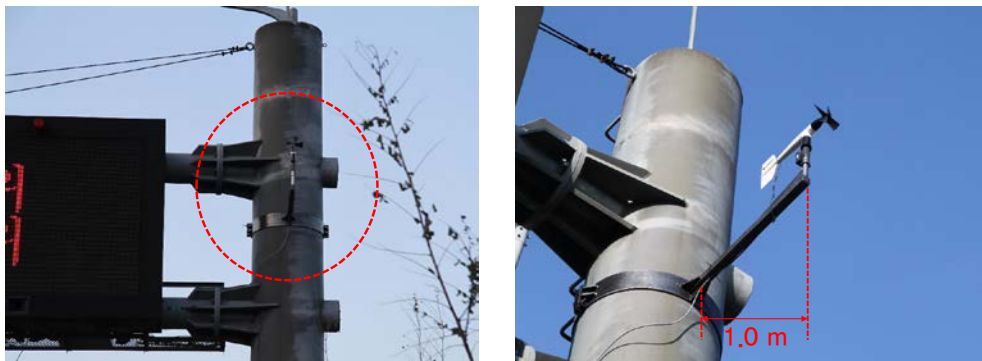


Fig. 3.12 Pictures of the installed anemometer

An anemometer was installed at the same height at the middle of the VMS as shown in Fig. 3.12. It was installed 1 m in front of the column in order to minimize interference by the VMS structure. The anemometer measured wind velocity that blows only in the vertical direction relative to the VMS

CHAPTER 4

CHARACTERISTICS OF TRUCK-INDUCED GUSTS

4.1 Wind pressure of truck-induced gusts

Six wind pressure sensors were analyzed in order to understand the characteristics of truck-induced gusts. When trucks pass beneath the VMS structure, pressure sensors installed in front of the VMS as well as pressure sensors that are installed at the bottom of the VMS responded to truck-induced gusts and the value of wind pressure measured by the wind pressure sensor installed in front of the VMS corresponds to about 65% of the value of wind pressure measured by the wind pressure sensor installed at the bottom of the VMS. In particular, a negative wind pressure occurs when trucks pass beneath the VMS structures. Therefore, if a negative wind pressure larger than -10 Pa was measured, this indicates that trucks passed in the other analysis as shown in both Fig. 4.1 and Fig 4.2. Wind pressure sensors 1, 2 and 3 shown in both Fig. 4.1 and Fig. 4.2 are expressed in Fig. 4.3. The wind pressure sensors 1 and 2 were installed at the bottom of the VMS and the wind pressure 3 is installed on the front of the VMS.

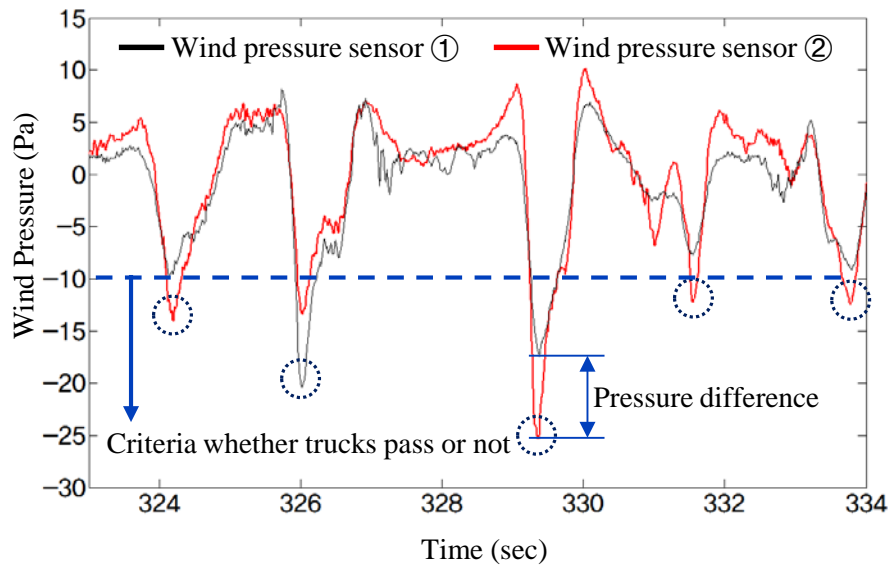


Fig. 4.1 Time history of wind pressures installed on the front of the VMS

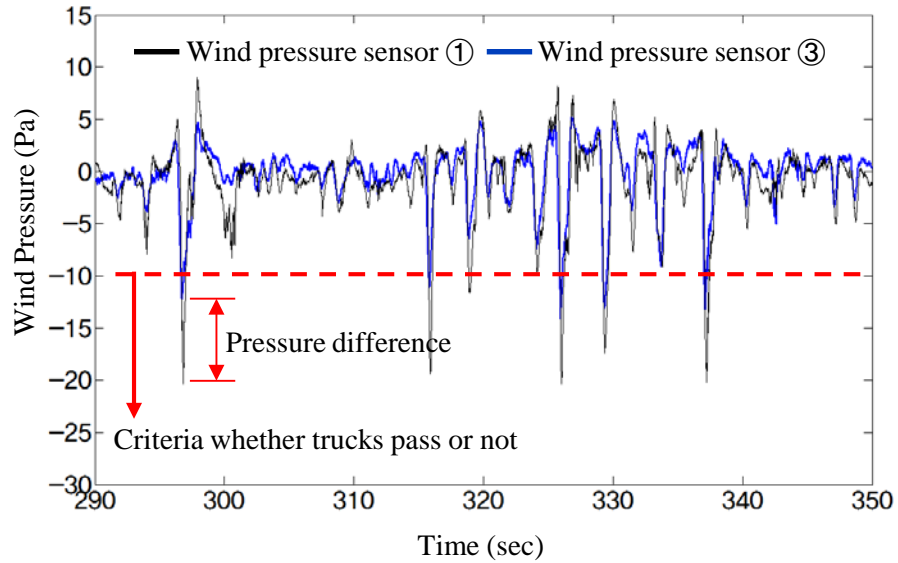


Fig. 4.2 Time history of wind pressures installed at the bottom of the VMS and on the front of the VMS

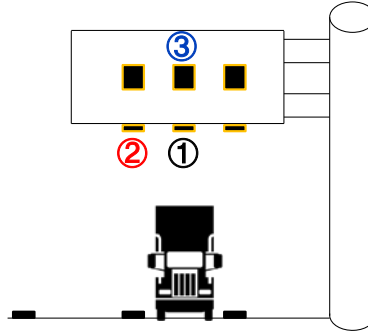


Fig. 4.3 Wind pressure sensor 1, 2 and 3

The above characteristics of wind pressure were used in order to distinguish them from the results of the strain gauges. Although the wind pressure applied in the front of the VMS was 35% less than the wind pressure applied at the bottom of the VMS, the cross-section area of the front of the VMS is 4.6 times larger than cross-sectional area of the bottom VMS.

4.2 Distribution of truck-induced gusts

The reduction in wind pressure ratio from the point where truck-induced gusts were generated was analyzed according to the distance from the point. This analysis was carried out by dividing into two cases shown in Fig. 4.4.

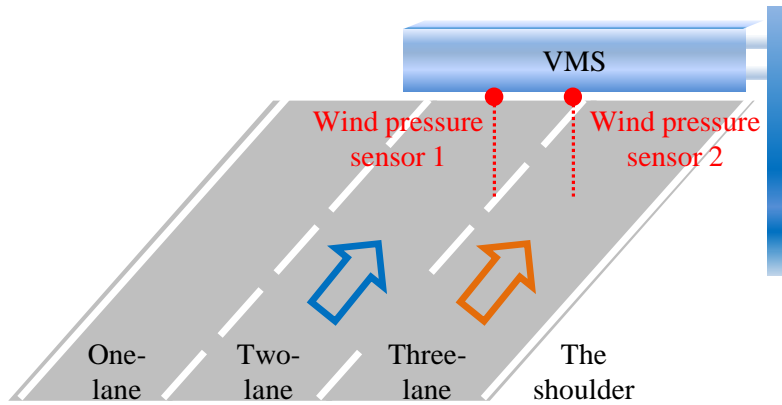


Fig. 4.4 Description of the two case for analyzing distribution of truck-induced gusts

One case is that when a truck passes beneath the VMS structure through three-lane (i.e. the orange arrow in Fig. 4.4), wind pressure reduction ratio through pressure sensors between above three-lane and above midpoint of both two-lane and three-lane. Among the many cases that trucks pass the beneath the VMS structure, trucks that pass through three-lane were detected by using the pressure sensor installed above three-lanes. For example, although all wind pressure sensors responded to truck-induced gusts, the value of sensor above the three-lane is always bigger than value for the other sensors. The other case is that when a truck passes beneath the VMS structure through a two-lane (i.e. the blue arrow in Fig. 4.4), wind pressure reduction ratio through the pressure sensors between above the two-lane and above the midpoint of both the two-lane and three-lane. Among the many cases where trucks pass the beneath the VMS structure, trucks that pass

through the two-lane were detached by using the pressure sensor installed above the two-lane.

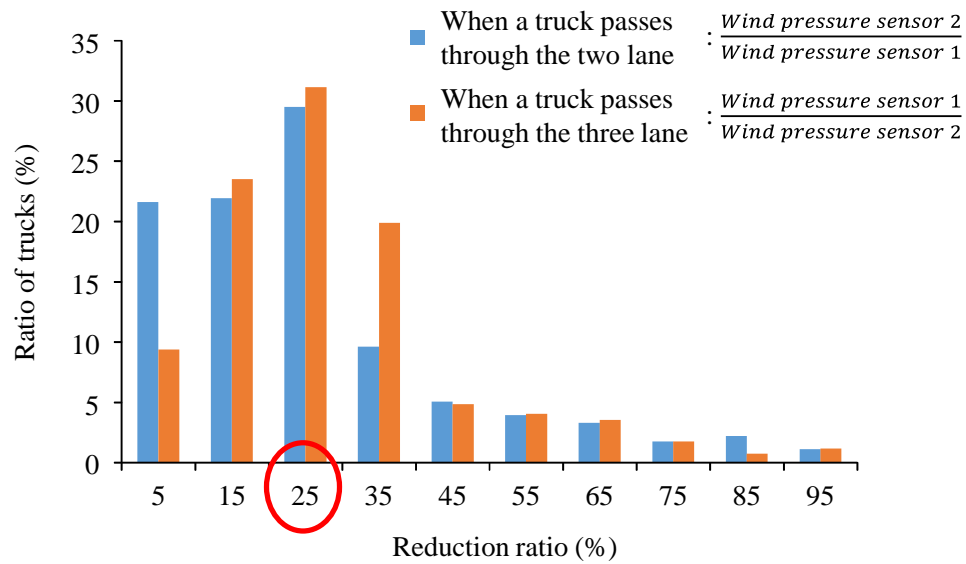


Fig. 4.5 Reduction ratio of wind pressure when a truck passes beneath the VMS structure

Two cases show that 25 % wind pressure reduction ratio is occurred most frequently as shown in Fig. 4.5.

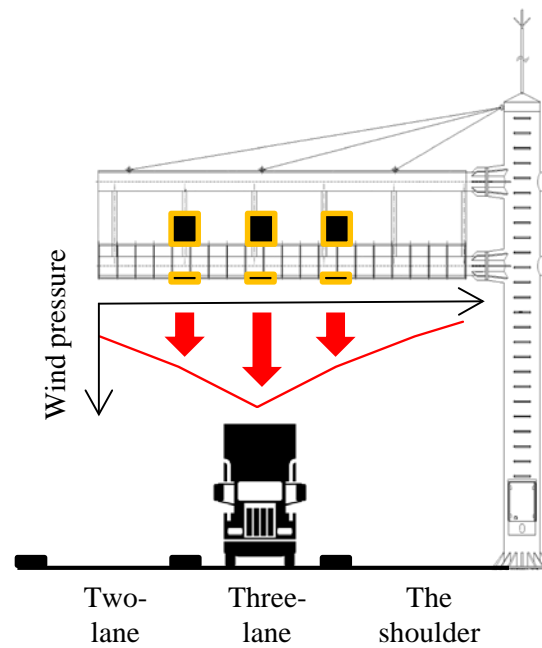


Fig. 4.6 Example for distribution of wind pressure occurred by truck-induced gusts

In other words, wind pressure occurred by a passing truck is decreased by 25 % for every 1.8 m around the passing truck as shown in Fig. 4.6.

CHAPTER 5

FATIGUE ASSESSMENT

5.1 Rainflow counting algorithm

The rainflow counting algorithm (S.D. Downing and D. F. Socie, 1982) was used for calculating the fatigue stress range from measured strain gauge data. It is useful to access the fatigue life of a structure subjected to a complex loading. Although it was first developed in 1968, Downing and Socie created the most commonly used rainflow counting algorithm in 1982.

This algorithm of rainflow counts a measured stress history of peaks and valleys in sequence. Rainflow counting algorithm is as the following steps (S.D. Downing and D. F. Socie 1982).

- 1) Read the next peak or valley
(if out of data, STOP)
- 2) Form ranges X and Y
(if the vector contains less than 3 points, go to the step 1)
- 3) Compare ranges X and Y
 - a. If $X < Y$, go to the step 1
 - b. If $X \geq Y$, go to the step 4

4) Count range Y, discard the peak and valley of Y, go to the step 2

X is range under consideration and Y is previous range adjacent to X.

5.2 Nominal stress point

It is necessary to find the nominal stress point because the AASHTO suggests that the threshold stress represents the nominal stress. Before the field tests, an FEM analysis based on three-dimensional elements was performed in order to check the stress distribution obtained from measured data and find the nominal stress point.

In the beginning, the program requires a partial modeling of the VMS structures in order to perform the analysis. The VMS structure, except for the column, was modeled using ABAQUS and the end of the mast arms connected to column was modeled as the fixed end. The load was applied to the bottom of the VMS as a uniformly distributed load. Stress concentration appeared up to about 200 mm from the stiffeners as shown in Fig. 3.11 and a constant stress was generated at a distance of at least 200 mm from the stiffener.

Measured stresses were estimated in order to find the nominal stress point. On the basis of the stress measured at a distance of 200 mm away from the stiffeners, the stress ratio of the other measured stresses were estimated and the results are shown in Fig. 5.1 And Fig. 5.2 explains the distance from the stiffeners

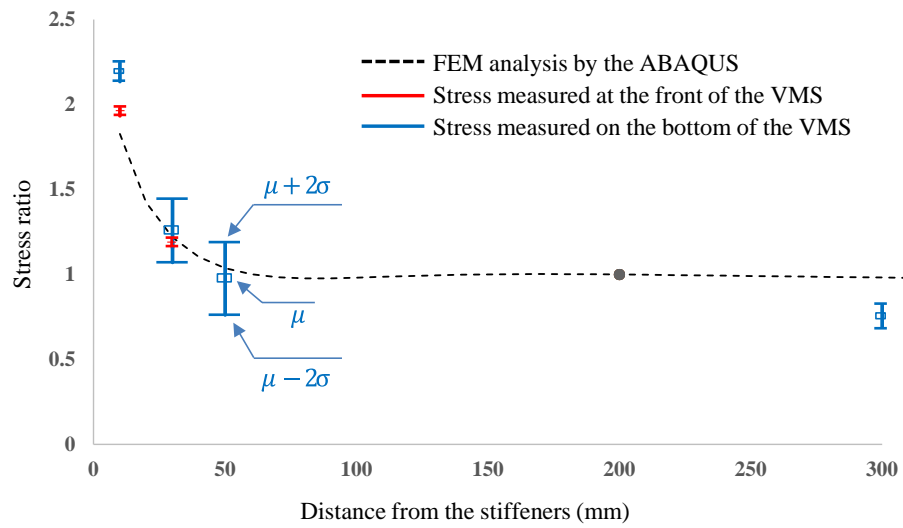


Fig. 5.1 Stress ratio according to the distance from the stiffeners

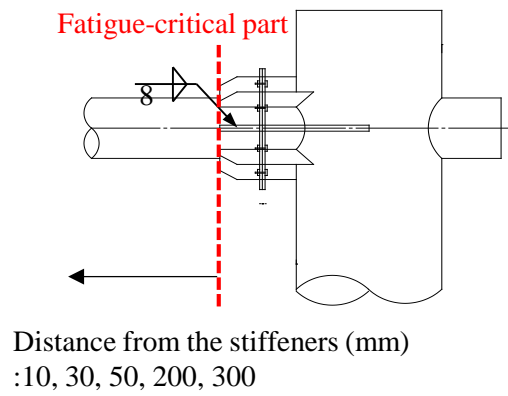


Fig. 5.2 Description about the distance from the stiffeners

FEM analysis results were also estimated by calculating the stress ratio on the basis of the measured stress in the 200 mm away from the stiffeners and measured stresses were compared with FEM analysis results.

Stresses measured closer than 200 mm from the stiffener showed a stress concentration and measured stresses 10 mm away from the stiffeners were about twice larger than the stresses that were measured 200 mm away from the stiffeners. These results are slightly larger than the FEM analysis results. Results measured 30 mm and 50 mm away from the stiffener are similar to the FEM analysis results. The results farther than 200 mm away from the stiffeners show consistent stresses and the results measured 200 mm away from the stiffeners were regarded as a nominal stress. 200 mm corresponds to both a half of an outer diameter of the mast arm and the result of the NCHRP Project 10-70.

5.3 Measurement result

Using previous analysis results regarding the nominal stress point, the fatigue stress range was calculated by means of a rain-flow algorithm and stresses measured 200 mm away from the stiffeners were utilized for estimating the fatigue stress range. The maximum fatigue stress range measured during the field tests was 9.3 MPa which was measured on the front of the mast arm.

Fatigue stress range measured on the front of the mast arm belonged to 1 MPa – 5 MPa and was mostly less than 3 MPa as shown in Fig. 5.3. Fatigue stress range measured at the bottom of the mast arm was mostly less than 2 MPa and the

maximum stress range measured during the field tests was 1.8 MPa as shown in Fig. 5.4.

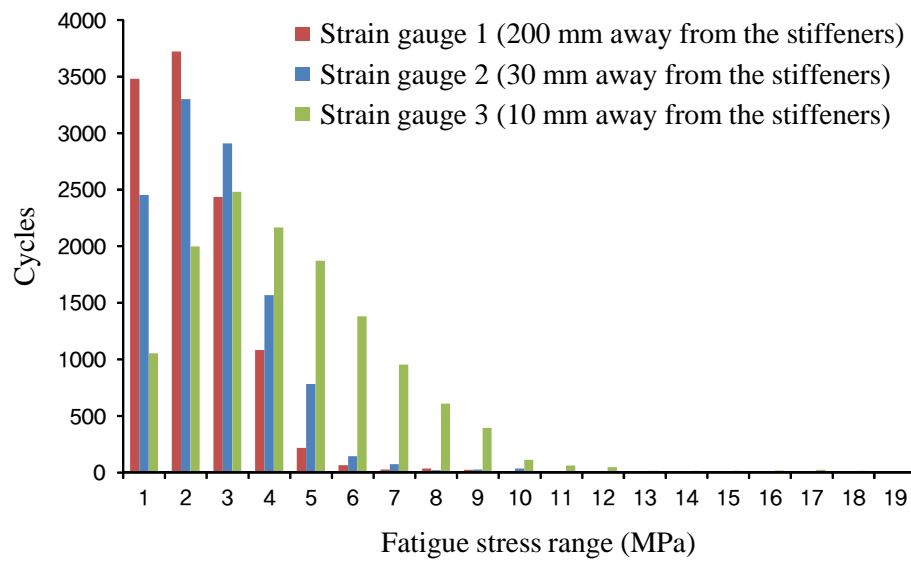


Fig. 5.3 Cycles of fatigue stress ranges measured on the front of the mast arm

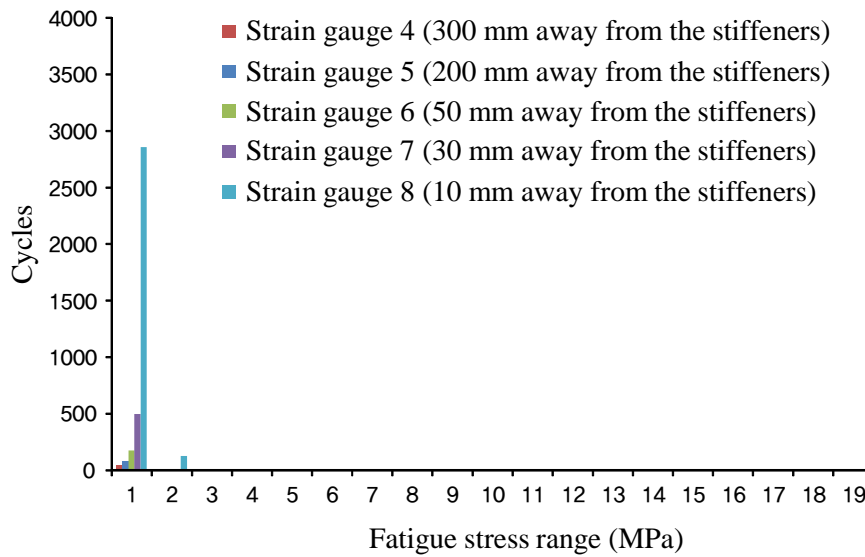


Fig. 5.4 Cycles of fatigue stress ranges measured at the bottom of the mast arm

Although the fatigue stress range measured on the front of the mast arm was bigger than that measured at the bottom of the mast arm, all of the fatigue stress range was less than the threshold stress recommended by the AASHTO. Because on the days when fatigue stress range was measured, there was almost no wind, fatigue stress range resulted from truck-induced gusts. In other words, all of the fatigue stress range measured during the field tests due to truck-induced gusts did not exceed the threshold stress.

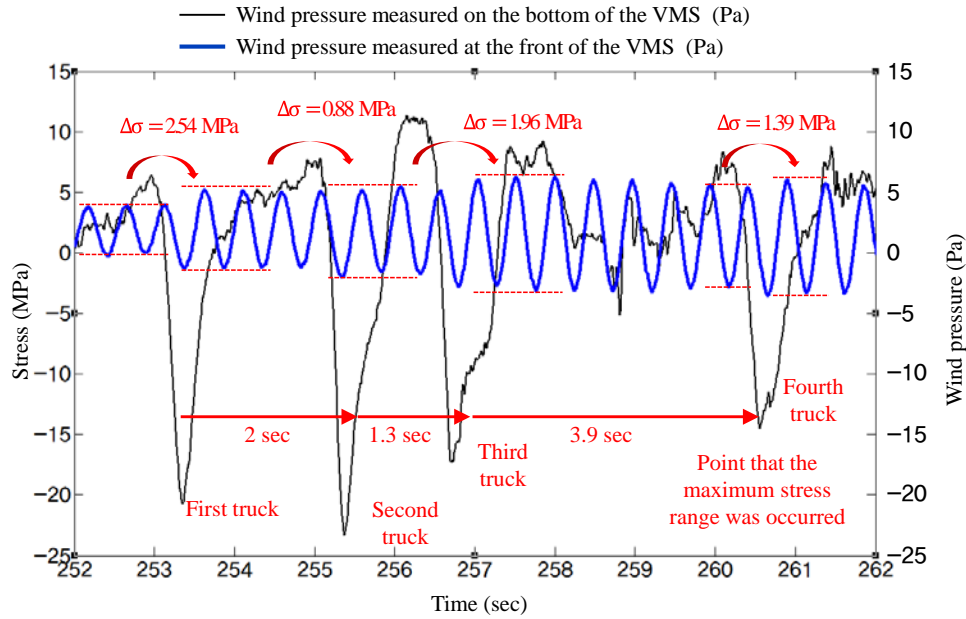


Fig. 5.5 Time history graph of sensors when the maximum stress range was occurred

A time history analysis was performed regarding the maximum fatigue stress range due to truck-induced gusts as shown in Fig. 5.5. Fig. 5.5 shows both wind pressure and fatigue stress of the front of the VMS during the 10 seconds near the occurrence of the maximum stress range.

Four trucks passed beneath the VMS structure in this time period and the time interval between the first truck and the last truck was about 7.2 seconds. The fatigue stress range was increased during these 7.2 seconds whenever a truck passed beneath the VMS structure and the maximum fatigue stress range occurred after the fourth truck passed. In other words, this maximum fatigue stress range due

to truck-induced gusts accumulated while trucks were continuously passing.

5.4 Verification of the distribution of truck-induced gusts

Previously analyzed distribution of truck-induced gusts was verified by comparison between fatigue stress ranges calculated from wind pressure sensor and strain gauge. Fig. 5.6 shows wind pressure of the bottom of the VMS and fatigue stress of both the front of the VMS and the bottom of the VMS during 70 seconds.

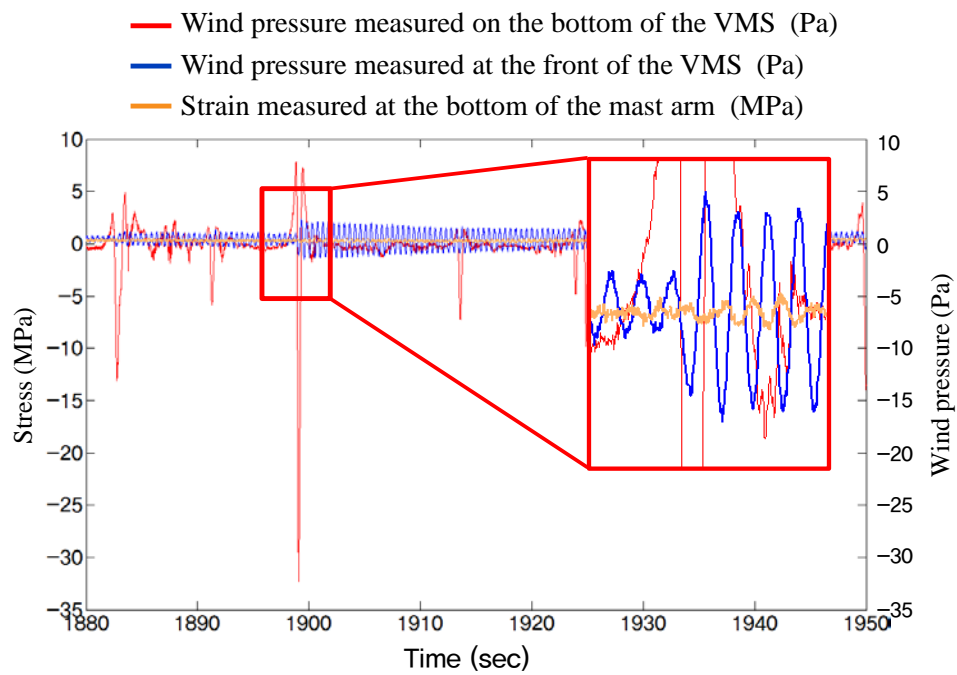


Fig. 5.6 Time history data used for verification of distribution of truck-induced gusts

The fatigue stress and wind pressure that was measured when a truck passed beneath the VMS structure was used for calculating the fatigue stress range and this moment is expressed as a red box in the Fig. 5.6. The previously analyzed distribution of truck-induced gusts was also applied in the calculation process and the result are shown in Table. 5.1.

Table 5.1 Result of fatigue stress range calculated from two sensors

Category	Calculation of fatigue stress range		Error (%)
	From wind pressure	From strain gauge	
Bottom of the VMS	0.43	0.42	2.3
Front of the VMS	0.83	2.2	-62.1

The fatigue stress range calculated from wind pressure which occurs at the bottom of the VMS is 0.43 MPa and from strain gauge is 0.42 MPa. These two results are almost the same, as the error between the two results is 2.3 %. However, the fatigue stress range generated in the front of the VMS which was calculated from the two sensors has 62.1 % error unlike the results from the bottom of the VMS.

Fatigue stress ranges calculated using wind pressure sensor data and strain gauge data were 0.83 MPa and 2.2 MPa, respectively. The negative wind pressure that occurred at the rear of the VMS was determined to be the cause of the different

fatigue stress ranges. These phenomena are similar with the end-effect shown in soundproof walls or wind barriers that increase wind velocity. Therefore, the wind pressure used for estimating the fatigue stress range was less than the wind pressure actually applied to the VMS and this accounts for the different fatigue stress range between two results.

CHAPTER 6

COMPARISON BETWEEN AASHTO AND MEASUREMENT RESULTS

6.1 Equivalent static gust pressure of both the front and bottom surface

Measured fatigue stress range was compared with the AASHTO design value as equivalent static gust pressure and the results are shown in Table. 6.1.

Table 6.1 Comparison between measured results and the AASHTO design value

Category	Measurement result		AASHTO design value	
	Maximum fatigue stress range	Equivalent static pressure	Truck-induced gusts	Natural wind gusts
Bottom of the VMS	1.8 MPa	370 Pa	1530 Pa	-
Front of the VMS	9.6 MPa	427 Pa	-	425 Pa

1.8 MPa which is the maximum fatigue range at the bottom of the mast arm measured during field tests was transformed as equivalent static gust pressure. In other words, equivalent static gust pressure which creates 1.8 MPa at the bottom of

the mast arm was inversely calculated. In the calculation process, it is assumed that equivalent static gust pressure was only applied to the width of one lane and speed of a truck is 108 km/h.

1.8 MPa corresponds to an equivalent static gust pressure of 370 Pa, about a quarter of the 1530 Pa recommended AASHTO design value for truck-induced gusts. This design value is four times larger than the inversely calculated equivalent static gust pressure obtained from measured results. The overestimated AASHTO design value has one thing in common with the previous studies.

Unlike the result of the bottom of the mast arm, 9.6 MPa measured on the front of the mast arm was compared with the AASHTO design value for natural wind gusts because truck-induced gusts suggested by the AASHTO are only applied to a horizontal surface of the attachment. In the calculation process, it is assumed that the wind velocity is 5 m/s and 9.6 MPa corresponds to an equivalent static gust pressure of 427 Pa, nearly the same as the 425 Pa suggested by the AASHTO specification for natural wind gusts. 9.6 MPa was due to truck-induced gusts and this result mentions that truck-induced gusts should be considered to vertical surface of the attachment.

CHAPTER 7

Further studies

7.1 Wind pressure of the VMS rear surface

Through verification for wind pressure of truck-induced gusts, it was confirmed that wind pressure occurred of the VMS rear surface increases wind pressure applied to front of the VMS. However, wind pressure applied to front of the VMS was only measured during the field tests. These phenomena are similar to the end-effect shown in soundproof walls or wind barriers that increase wind velocity. These structures have in common the fact that the VMS depth in the direction that the wind is blowing is relatively shorter than the length of the VMS. Therefore, the drag coefficients for structures like soundproof walls or wind barriers are appear to be different according to the ratio of height and length. For example, these negative wind pressures occurred at the rear of the VMS, resulting in larger drag coefficients by 2 times. If additional field tests would to be carried out, it would be necessary to install wind pressure sensors at the rear of the VMS.

7.2 Fatigue assessment about natural wind gusts

During the field tests, the measured maximum wind velocity was less than 3 m/s and the measured mean wind velocity was less than 1 m/s. Therefore, the measured fatigue stress ranges are mostly generated due to truck-induced gusts.

Although wind pressure in a direction vertical to the VMS generates the maximum fatigue stress range, wind pressure not in the direction vertical to the VMS can also actually generate fatigue stress. However, because the installed anemometer could only measure the wind velocity in a direction vertical to the VMS, the effects of natural wind gusts would be underestimated. Moreover, if truck-induced gusts are overlapped with natural wind gusts, fatigue stress range will be increased.

CHAPTER 8

CONCLUSIONS

The following conclusions can be made based on the obtained results:

1. The field tests were carried out in order to evaluate the characteristics of truck-induced gusts because it is hard to simulate truck-induced gusts in wind-tunnel tests. The target of the field tests was selected as a VMS structure on the highway which is known as the type of structure that is most affected by truck-induced gusts. The site of the field tests was the highway where vehicle speed is usually higher than in other sites.
2. Truck-induced gusts are applied to not only the vertical direction but also the horizontal direction. In particular, the maximum fatigue stress range was measured on the front of the mast arm. Unlike the AASHTO assumptions for truck-induced gusts, truck-induced gusts should be considered about both vertical and horizontal directions.
3. Truck-induced gusts are applied to not width of one lane but entire width of the VMS. And wind pressure occurred due to truck-induced gusts is reduced by 25 % for every 1.8 m (i.e. half of a lane width) around the

passing truck. This distribution is also applied to the front of the VMS as well as the bottom of the VMS but also.

4. All of the measured fatigue stress ranges were less than the threshold stress recommended by the AASHTO. And the fatigue stress range measured at the bottom of the mast arm corresponds to a quarter of the equivalent static truck gust pressure range recommended by the AASHTO and this result is consistent with data published in previous studies. In other words, the truck-induced gusts suggested by the AASHTO are overestimated. However, because during the field tests there were days when the wind almost did not blow, fatigue stress can be largely attributed to truck-induced gusts. Therefore, if natural wind gusts can increase effects of truck-induced gusts, a parametric study about natural wind gusts should be carried out in order to understand the overlapping effects between truck-induced gusts and natural wind gusts.

REFERENCES

- AASHTO (2013). Standard specifications for structural supports for highway signs, luminaires, and traffic signals.
- Albert, M. N., Manuel, L., Frank, K. H., & Wood, S. L. (2007). Field testing of cantilevered traffic signal structures under truck-induced gust loads: Center for Transportation Research, University of Texas at Austin.
- Dexter, R. J., & Ricker, M. J. (2002). *Fatigue-resistant design of cantilevered signal, sign, and light supports*: Transportation Research Board.
- DMRB (2007). Highway structures : design(sub-structures and special structures), materials.
- Downing, S. D., & Socie, D. (1982). Simple rainflow counting algorithms. *International Journal of Fatigue*, 4(1), 31-40.
- EUROCODE (2005). tions on structures.
- Florea, M. J., Manuel, L., Frank, K. H., & Wood, S. L. (2007). Field tests and analytical studies of the dynamic behavior and the onset of galloping in traffic signal structures.
- Hobbacher, A. (2009). *Recommendations for fatigue design of welded joints and components*: Welding Research Council Shaker Heights, OH.
- Johns, K. W., & Dexter, R. J. (1998). Fatigue related wind loads on highway support structures.
- Kaczinski, M. R., Dexter, R. J., & Van Dien, J. P. (1998). *Fatigue-resistant design*

of cantilevered signal, sign and light supports: Transportation Research Board.

Roy, S., Park, Y., Sause, R., Fisher, J., & Kaufmann, E. (2011). *Cost-effective connection details for highway sign, luminaire, and traffic signal structures*: National Cooperative Highway Research Program, Transportation Research Board of the National Academies.

Wieghaus, K. T., Hurlebaus, S., Mander, J. B., & Fry, G. T. (2014). Wind-induced traffic signal structure response: Experiments and reduction via helical arm strakes. *Engineering Structures*, 76, 245-254.

Zuo, D., Smith, D. A., & Mehta, K. C. (2014). Experimental study of wind loading of rectangular sign structures. *Journal of Wind Engineering and Industrial Aerodynamics*, 130, 62-74.

손용춘, 임종국, & 유경아. (2008). 도로전광표지판 (VMS) 의 내풍성능 향상에 관한 연구. *한국풍공학회 학술발표회논문집*, 199-204.

국 문 초 록

이 연구에서는 차량이 표지판, 신호등과 같은 지주구조물을 통과하면서 발생하는 트럭풍 거스트가 구조물에 발생시키는 피로 응력을 평가하였다. 풍동 실험을 통해서도 트럭풍 거스트를 모사하기 힘든 연구의 한계점을 고려하여, 현장계측을 통해서 본 연구를 수행하였다. 또한, AASHTO에서 언급되는 것과 같이 트럭풍 거스트의 영향을 가장 많이 받는 하부 단면적이 큰 구조물인 VMS (Variable message sign)을 대상으로 현장계측을 수행하였다.

구조물의 피로취약부인 VMS 하부 마스트암을 중점으로 총 3종류의 센서를 활용하여 현장계측을 수행하였다. 하부 마스트암의 전면부와 하면부에 각각 3개, 5개의 변형률계를 설치하여 피로 응력 범위를 평가하였다. 또한, VMS 전면부와 하면부에 각각 3개의 압력센서를 설치하여 트럭풍 거스트의 특성을 파악하였고, VMS 높이와 동일선 상에 풍속계를 설치하여 트럭풍 거스트와 자연풍 거스트의 영향을 분간하는데 활용하였다.

측정된 공칭응력은 Rainflow counting 알고리즘을 활용하여 피로 응력 범위로 산정하였으며, AASHTO에서 상세 별로 제시하고 있는 피로 저항강도와 비교하였다. 그리고 풍압센서를 통해 분석된 트럭풍 거스트의 특성은 압력센서와 변형률계를 통해서 검증하였다.

또한, 측정된 피로 응력 범위를 AASHTO에서 피로 설계 시 제시하는 등가의 정적 풍압과 비교하였다. 즉, 마스트암 전면부와 하면부에서 측정된 피로 응력 범위가 산정되는 등가의 정적 풍압을 계산하고 이를 각각 AASHTO에서 제시하는 자연풍 거스트 산정식과 트럭풍 거스트 산정식과 비교하였다.

현장계측 기간 동안에는 고풍속의 바람이 불지 않아 트럭풍 거스트의 영향만을 평가하였다. 하지만, 고풍속의 바람으로 인한 자연풍 거스트의 영향이 트럭풍 거스트에 중첩되어 더 큰 피로 응력을 발생시킨다면, 이에 대한 효과를 정확히 평가하기 위해서는 추후 구체적인 분석이 더 필요함을 알 수 있었다.

주요어: 피로 평가, 트럭풍 거스트, 현장 계측, 지주구조물, Rainflow counting algorithm

Student Number: 2013-20948